

ORIGINAL ARTICLE

The AP-1 transcription factor FOSL1 causes melanocyte reprogramming and transformation

K Maurus^{1,2}, A Hufnagel¹, F Geiger¹, S Graf³, C Berking³, A Heinemann⁴, A Paschen⁵, S Kneitz¹, C Stigloher⁶, E Geissinger², C Otto⁷, A Bosserhoff^{8,9}, M Scharlt^{1,10,11} and S Meierjohann^{1,10}

The MAPK pathway is activated in the majority of melanomas and is the target of therapeutic approaches. Under normal conditions, it initiates the so-called immediate early response, which encompasses the transient transcription of several genes belonging to the AP-1 transcription factor family. Under pathological conditions, such as continuous MAPK pathway overactivation due to oncogenic alterations occurring in melanoma, these genes are constitutively expressed. The consequences of a permanent expression of these genes are largely unknown. Here, we show that FOSL1 is the main immediate early AP-1 member induced by melanoma oncogenes. We first examined its role in established melanoma cells. We found that FOSL1 is involved in melanoma cell migration as well as cell proliferation and anoikis-independent growth, which is mediated by the gene product of its target gene *HMGA1*, encoding a multipotent chromatin modifier. As FOSL1 expression is increased in patient melanoma samples compared to nevi, we investigated the effect of enhanced FOSL1 expression on melanocytes. Intriguingly, we found that FOSL1 acts oncogenic and transforms melanocytes, enabling subcutaneous tumor growth *in vivo*. During the process of transformation, FOSL1 reprogrammed the melanocytes and downregulated MITF in a *HMGA1*-dependent manner. At the same time, AXL was upregulated, leading to a shift in the MITF/AXL balance. Furthermore, FOSL1 re-enforced pro-tumorigenic transcription factors MYC, E2F3 and AP-1. Together, this led to the enhancement of several growth-promoting processes, such as ribosome biogenesis, cellular detachment and pyrimidine metabolism. Overall, we demonstrate that FOSL1 is a novel reprogramming factor for melanocytes with potent tumor transformation potential.

Oncogene advance online publication, 8 May 2017; doi:10.1038/onc.2017.135

INTRODUCTION

Melanoma belongs to the tumor entities with the highest genomic instability and plasticity. Despite large inter-individual genomic differences, melanomas share common features, such as high activities of certain signaling pathways, which are caused by oncogenes or epigenetic mechanisms. Most strikingly, a large majority of melanomas shows a strong activation of the ERK1/2 pathway.¹ Physiologically, this pathway is activated in a directed and well-regulated manner, for example, after ligand-dependent stimulation of receptor tyrosine kinases. This leads to the transient expression of 'immediate early' genes, whose increased transcription is only measurable for a few hours and then goes back to background levels. However, when the ERK1/2 pathway is constitutively active, for example, by activating mutations in BRAF and NRAS, these 'immediate early' genes are expressed at increased rates.

Various transcription factors of the AP-1 family of basic region leucine zippers (bZIP) are among the 'immediate early' genes. They are able to induce a secondary set of potentially tumor-relevant genes and thereby strongly influence the epigenetic landscape.

AP-1 transcription factors are composed of members of the JUN, FOS, ATF/CREB and MAF families. JUN and FOS are the best investigated AP-1 members and comprise the first identified oncogenic transcription factors.² JUN is involved in melanoma tumorigenesis, plasticity and resistance,^{3,4} and high JUN levels are maintained by E-cadherin loss, RhoC activity or the documented reduction of miR125 in melanoma.^{5–7} JUN family members can either homodimerize or form heterodimers with FOS, ATF/CREB or MAF family proteins. The FOS family is comprised of FOS, FOSB, FOSL1 and FOSL2, all of which are classified as immediate early genes.^{8–10} Together with their JUN family dimerization partners, FOS family members bind preferentially to the tetradecanoylphorbol acetate (TPA)-responsive element with the heptamer consensus sequence 5'-TGA(C/G)TCA-3'.¹¹ Although the AP-1 transcription factor is involved in mediating pro-tumorigenic events, this effect is context-dependent, and tumor suppression by AP-1 was also observed, for example, the apoptosis-promoting function of JUN in UV-irradiated fibroblasts¹² or FOSB in breast cancer.¹³ The function of the FOS family members was described for different cancer types, and the existing data suggest that some of them are

¹Department of Physiological Chemistry, University of Würzburg, Würzburg, Germany; ²Institute of Pathology, University of Würzburg, Würzburg, Germany; ³Department of Dermatology and Allergy, Munich University Hospital (LMU), Munich, Germany; ⁴Division of Immunology, Paul-Ehrlich Institute, Langen, Germany; ⁵Department of Dermatology, University Hospital Essen, University Duisburg-Essen and German Cancer Consortium (DKTK), Partner Site Essen/Düsseldorf, Essen, Germany; ⁶Department of Cell and Developmental Biology, Division of Electron Microscopy, University of Würzburg, Würzburg, Germany; ⁷Experimental Surgery, Department of General, Visceral, Vascular, and Pediatric Surgery, University Hospital of Würzburg, Würzburg, Germany; ⁸Institute of Biochemistry, Emil-Fischer-Centrum, Friedrich Alexander University Erlangen-Nürnberg, Erlangen-Nürnberg, Germany; ⁹Comprehensive Cancer Center Erlangen-EMN, University of Erlangen, Erlangen, Germany; ¹⁰Comprehensive Cancer Center Mainfranken, University Hospital Würzburg, Würzburg, Germany and ¹¹Texas A&M Institute for Advanced Studies and Department of Biology, Texas A&M University, College Station, TX, USA. Correspondence: Professor S Meierjohann, Department of Physiological Chemistry, University of Würzburg, Biocenter, Am Hubland, Würzburg, 97074, Bavaria, Germany. E-mail: svenja.meierjohann@biozentrum.uni-wuerzburg.de

Received 1 September 2016; Received 31 March 2017; accepted 4 April 2017

tumorigenic. The alternatively spliced FOSB transcript form Δ FOSB causes quiescent cells to re-enter the cell cycle,¹⁴ and FOS is required for the malignant conversion of non-melanoma skin tumors.¹⁵ FOSL1 was hitherto described to be mainly involved in late tumor stages, as it promotes epithelial-to-mesenchymal transition and the accompanying promotion of invasion and metastasis, for example, in colorectal cancer and breast cancer.^{16–18} This is consistent with the physiological role of FOSL1 in the developing embryo, where it is responsible for trophoblast migration.¹⁹

Here, we demonstrate that melanoma oncogenes BRAF^{V600E} and NRAS^{Q61K} increase the transcription of *FOSL1* as the only gene among the immediate early AP-1 family members. We dissected its function in established melanoma cells and in benign melanocytes and found that FOSL1 plays a major role in melanocyte reprogramming by altering the balance between MITF and AXL and enforcing pro-tumorigenic transcription factors.

RESULTS

FOSL1 is the major immediate early family member induced by oncogenic BRAF and NRAS

To identify melanoma-relevant AP-1 family members, we generated normal human epidermal melanocytes (NHEM) transgenic for

doxycycline (Dox)-inducible BRAF^{V600E} or NRAS^{Q61K}. Oncogene expression and downstream ERK1/2 activation was induced. We tested the expression of all those AP-1 family members, which are known immediate early genes (*JUN*, *FOS*, *FOSB*, *FOSL1*, *FOSL2*) (Figures 1a and b). *FOSL1* was the only gene significantly upregulated by NRAS^{Q61K} and BRAF^{V600E}. Next, we addressed the regulation of *FOSL1* in human melanoma cell lines using inhibitors blocking the main pathways downstream of BRAF (MEK inhibitor PD184352) and NRAS (MEK inhibitor PD184352 and PI3K inhibitor GDC0941) (Figures 1c–f). The mutation status of melanoma oncogenes in these cell lines is shown in Supplementary Table 2. Notably, the PI3K pathway is frequently active in melanomas to some degree, for example, due to NRAS or PTEN mutations. Interestingly, both inhibitors were able to diminish FOSL1 expression on RNA and protein level to a similar extent, indicating that neither pathway alone is sufficient to maintain high FOSL1 levels. In primary NHEM, the PI3K inhibitor is also able to block the BRAF- or NRAS-induced increase of FOSL1 (Supplementary Figure 1A), thus showing that endogenous, oncogene-independent PI3K contributes to the FOSL1 levels.

In addition, FOSL1 is regulated by p53 in a miR-34a/c-dependent manner.¹⁸ To investigate the contribution of p53 to FOSL1 expression, we activated p53 by either SN-38, a topoisomerase inhibitor, or nutlin3a, an MDM2-dependent p53 activator, in the human melanoma cell line UACC62. SN-38 treatment resulted in an increased expression of miR-34a and

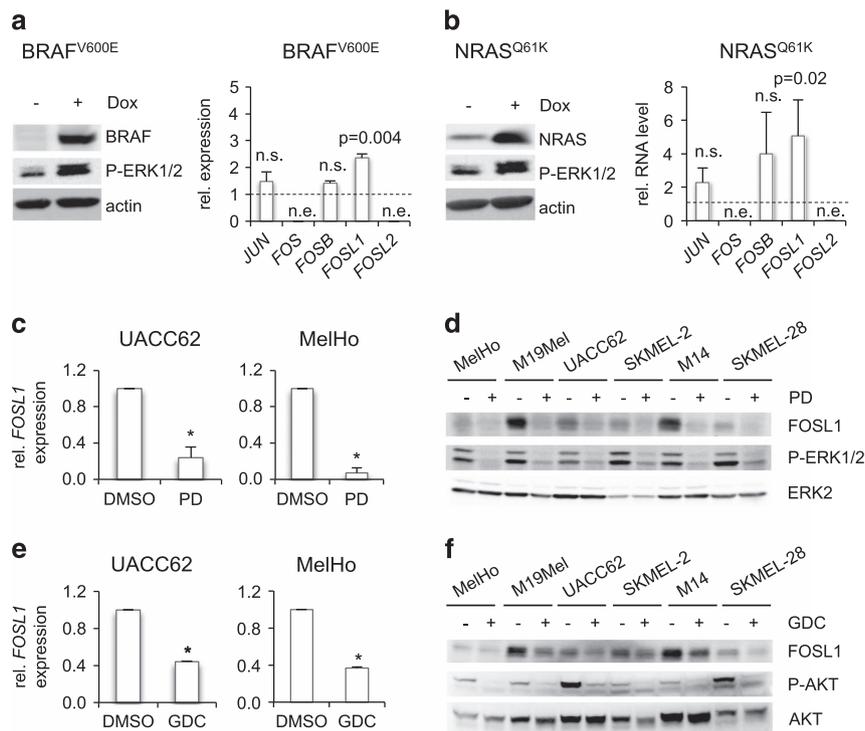


Figure 1. Expression of AP-1 family members in melanoma. **(a)** BRAF^{V600E}-dependent expression of AP1 transcription factors in NHEM cells expressing a Dox-inducible BRAF^{V600E} construct. Left: Protein blot showing expression of BRAF and induction of P-ERK1/2 (Thr202/Tyr204) in response to Dox treatment (50 ng/ml, 24 h). Actin served as loading control. Right: Corresponding relative expression levels of indicated genes, measured by real-time PCR. *RPS14* served as expression control. The graph shows the change in gene expression of Dox-treated cells compared to untreated cells (**P* < 0.05, ***P* < 0.01). **(b)** NRAS^{Q61K}-dependent expression of AP1 transcription factors in NHEM cells expressing a Dox-inducible NRAS^{Q61K} construct. The blot on the left shows the expression of NRAS and P-ERK1/2 in response to Dox treatment. The graphs on the right show the corresponding real-time results. All conditions are similar to those described in **(a)**. **(c)** Real-time PCR analysis of *FOSL1* gene expression after 24 h of MEK inhibition with 2 μ M PD184352 in UACC62 and MelHo cells. Calculations were made from two independent experiments, each performed in triplicates. **(d)** FOSL1 and P-ERK1/2 (Thr202/Tyr204) protein levels as readout for MEK inhibition of indicated human melanoma cell lines after 24 h of MEK inhibition with 2 μ M PD184352. ERK2 served as loading control. **(e)** Real-time PCR analysis of *FOSL1* expression after 24 h of PI3K inhibition with 5 μ M GDC0941 in UACC62 and MelHo cells. The experiment was performed twice, each time in triplicates. **(f)** FOSL1 and P-AKT (Ser473) levels in indicated human melanoma cell lines after 24 h of PI3K inhibition with 5 μ M GDC0941. Total AKT served as loading control. Please note that the strong AKT activation in UACC62 and SKMEL-28 cells is attributed to the reported PTEN mutations (http://cancer.sanger.ac.uk/cell_lines). The small background activation of AKT, as seen in the other cell lines, is likely the result of receptor tyrosine kinase engagement, for example, by ligands present in the serum.

miR-34c, while nutlin3a only induced miR-34c (Supplementary Figure 1B). Still, both agents led to p53 stabilization and the reduction of FOSL1, particularly after 72 h (Supplementary

Figure 1C). This delayed effect is most likely attributed to the fact that FOSL1 protein stability is enhanced by ERK1/2-dependent phosphorylation,²⁰ which occurs in UACC62 cells as a result

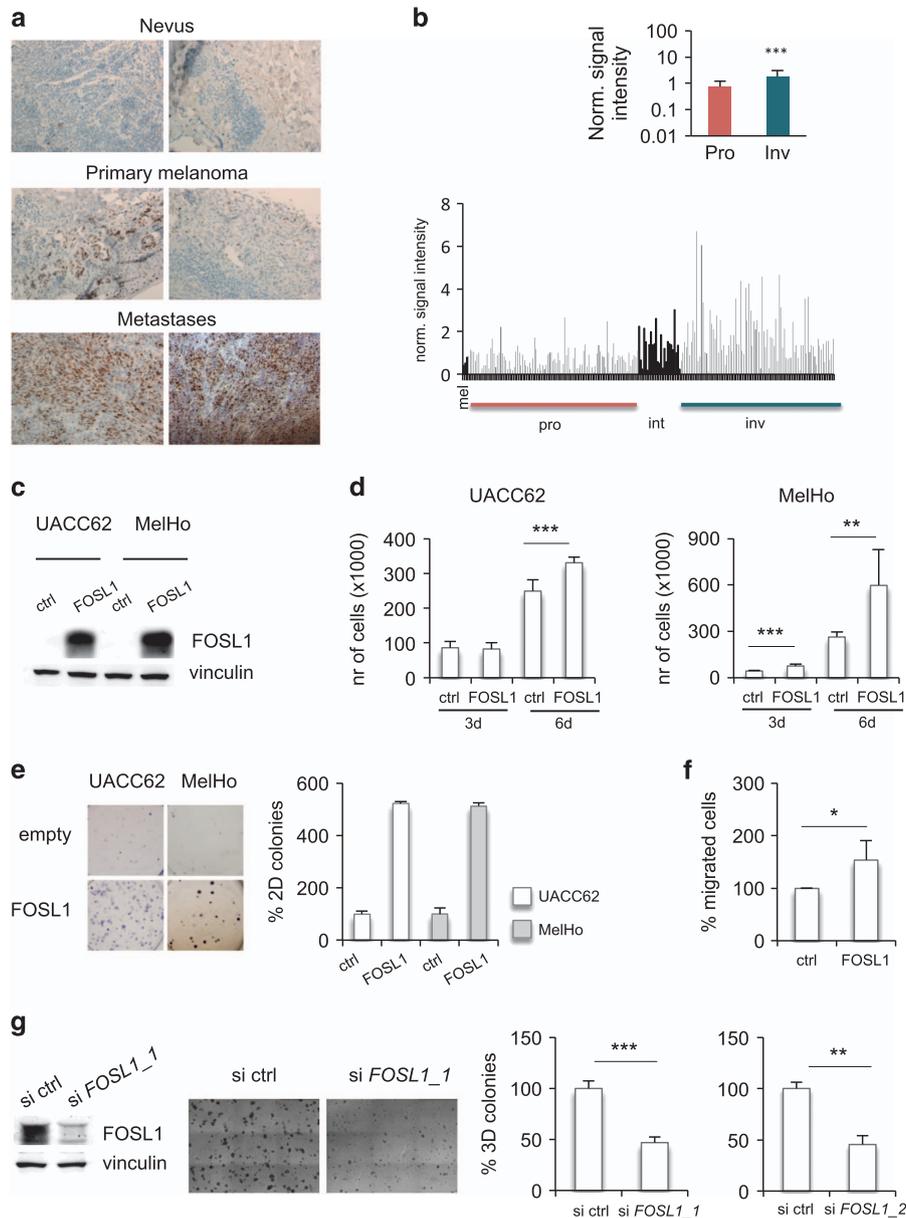


Figure 2. FOSL1 expression promotes pro-tumorigenic features in melanoma. **(a)** Representative images from a melanoma tissue microarray from human nevi, primary and metastatic melanoma. Brown staining indicates specific binding of FOSL1-specific antibody. **(b)** Classification of melanoma cells by phenotype-specific *FOSL1* gene expression according to Widmer *et al.*²⁴ Analysis of a prosubset of 220 samples of melanoma cell lines reveals average expression signals of 0.75 (± 0.49) and 1.8 (± 1.24) for FOSL1 in proliferative and invasive signature samples, respectively. This 2.4-fold difference is significant ($P < 1.00E-05$). Pro: proliferative, Int: intermediate, Inv: invasive. **(c)** Western blot analysis of FOSL1 in UACC62 and MelHo cells transfected with a constitutive FOSL1 expression vector (p201-FOSL1). Vinculin served as loading control. Please note that although the FOSL1 overexpression seems to be very strong in relation to endogenous FOSL1 (which is not visible in this comparison), the FOSL1 levels of transfected UACC62 and MelHo cells are comparable to those of melanoma cells with high endogenous FOSL1 (see Supplementary Figure 2A). **(d)** Proliferation assay of FOSL1 overexpressing and empty vector cells. Cells were manually counted at day 3 and 6 after plating. Calculations were made from two independent experiments, each performed in triplicates. **(e)** Colony formation assay. Cells were seeded at low density (400 cells/well of a 6-well dish for UACC62 cells, 150 cells/well for MelHo cells) and were cultivated for 12 days to allow the formation of visible colonies. Thereafter, wells were stained with 2% crystal violet solution and pictures were taken. The left image shows the pictures, the corresponding quantification is shown on the right. The experiment was done in triplicates and representative images are shown. **(f)** Transwell migration assay of control and FOSL1 overexpressing MelHo cells. Cells were allowed to migrate for 8 h. The assay was performed three times in triplicates. **(g, left):** Western blot of FOSL1 expression after siRNA mediated knockdown for 3 days, using smartpool siRNA (*FOSL1_1*). Vinculin served as a loading control. Middle: soft agar growth of UACC62 cells after treatment with control or *FOSL1* specific siRNA (*FOSL1_1*) and cultivation for 7 days. Right: associated quantification for the siRNA *FOSL1_1* and a second FOSL1-specific single siRNA (*FOSL1_2*). Experiments were performed two times in triplicates. * $P < 0.05$; ** $P < 0.01$; *** $P < 0.001$.

of BRAF^{V600E} expression. Similarly, miRNA mimics for miR-34a and miR-34c, but not miR-34b, reduced FOSL1 expression in melanoma cells (Supplementary Figure 1D), indicating that the p53-miR-34a/c-FOSL1 axis can be reactivated in melanoma. However, when comparing the relative contribution of MEK inhibition, PI3K inhibition and p53 activation on FOSL1 protein levels, the p53 pathway only played a minor role in reducing FOSL1 (Supplementary Figure 1E). Concludingly, FOSL1 is maintained through the joint activation of the RAF/MEK/ERK1/2 and the PI3K pathway in melanoma. Notably, an activated PI3K pathway is associated with melanoma progression and metastasis.^{21–23}

FOSL1 affects numerous pro-tumorigenic features in melanoma. To test the abundance of FOSL1 expression in human melanoma samples, FOSL1 staining of a melanoma tissue array including nevus, primary melanoma and metastases samples was performed. The staining revealed that FOSL1 staining is highest in metastases (Figure 2a and Supplementary Table 3). In addition, in a systematic phenotype-specific classification of 220 melanoma cell lines (according to HOPP analysis, as described in Widmer *et al.*,²⁴), FOSL1 expression is significantly associated with an invasive cell phenotype (Figure 2b).

FOSL1 is located on chromosomal region 11q13, which is frequently amplified in melanoma.²⁵ To test whether an increased

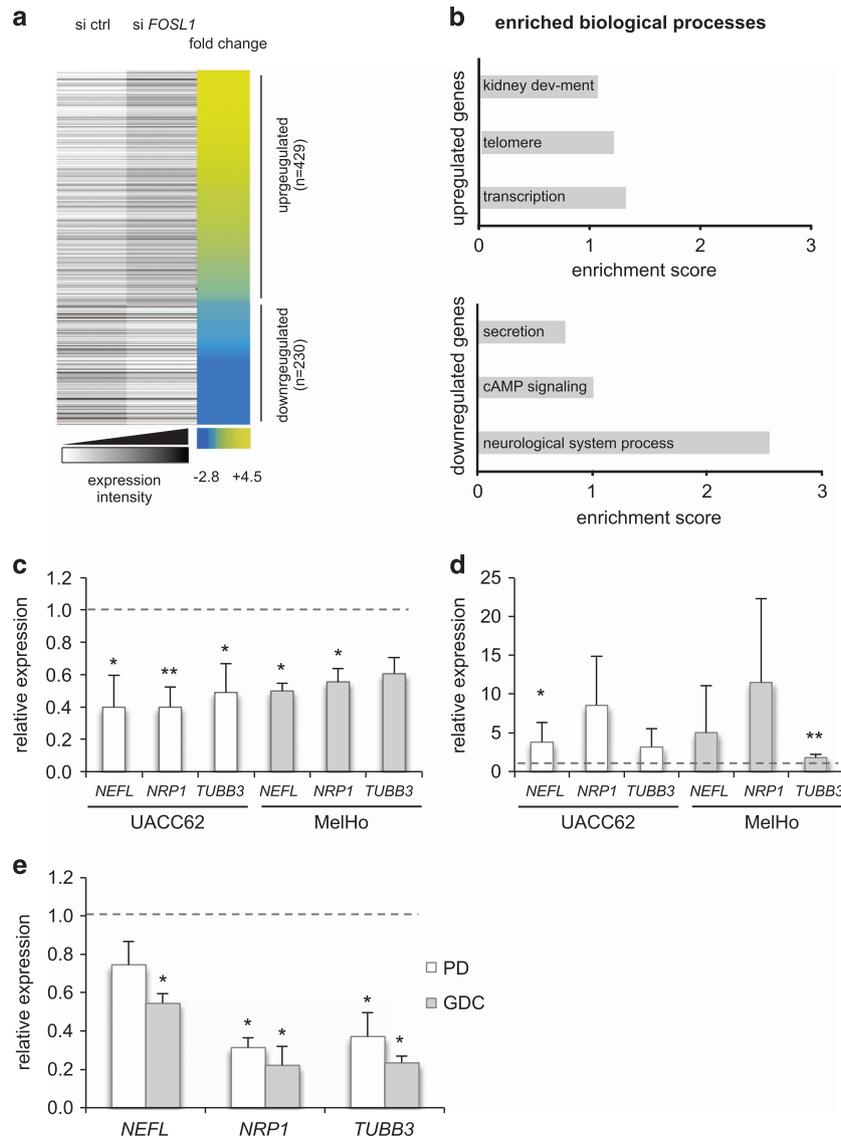


Figure 3. Gene regulation by FOSL1 in melanoma. **(a)** Heatmap of up- and downregulated genes after *FOSL1* siRNA treatment (fold change ≥ 1.5 , min log₂ Robust Multi-array Average signal intensity ≥ 6). Robust Multi-array Average signal intensities are shown in gray. Fold changes are shown in yellow-blue. **(b)** Graph showing the three most enriched biological processes for up- and downregulated genes. Values above an enrichment score of 1.3 are considered to be of biological relevance.⁴⁵ **(c)** Real-time PCR of indicated neuronal genes in UACC62 and MelHo cells after siRNA mediated knockdown of *FOSL1* for 3 days, using smartpool siRNA. Values for UACC62 cells were calculated from three different experiments performed in triplicates. Values for MelHo cells were calculated from two independent biological replicates. **(d)** Real-time PCR of neuronal genes in UACC62 and MelHo cells overexpressing *FOSL1* compared to control cells. Experiments were performed four times. Due to fluctuating overexpression of *FOSL1*, the degree of upregulation of the three target genes differed between the four experiments, and the results did not reach significance. However, in each single experiment, upregulation of the target genes was noted. **(e)** Real-time PCR analysis of *NEFL*, *NRP1* and *TUBB3* in UACC62 cells after treatment with 2 μ M MEK inhibitor PD184352 and 5 μ M PI3K inhibitor GDC0941 for 24 h. Calculations were made from two independent experiments, each done in triplicates. **P* < 0.05; ***P* < 0.01.

FOSL1 expression is beneficial for established melanoma cells, the two melanoma cell lines UACC62 and MelHo, with low intrinsic FOSL1 levels (see Figures 1d and f) were transfected with FOSL1 overexpression vector (Figure 2c). This led to a FOSL1 expression, which was in the range of cell lines containing high endogenous FOSL1, such as M19-Mel and M14 (Supplementary Figure 2A). In UACC62 and MelHo, FOSL1 caused increased proliferation (Figure 2d), and colony formation (Figure 2e). Furthermore, migration was significantly enhanced in MelHo-FOSL1 cells (Figure 2f). Migration of UACC62 cells was not analyzed, as their large cell size precluded the usage of standard transwell migration assays. Soft agar growth was not affected by *FOSL1* overexpression, but siRNA-mediated knockdown strongly reduced the number of soft agar colonies in UACC62 cells (Figure 2g).

Concludingly, FOSL1 affects numerous tumorigenic features in melanoma.

FOSL1 induces neuronal genes in melanoma cells

To get insight into the underlying processes of FOSL1 effects in melanoma, transcriptional regulation by FOSL1 in melanoma was studied. To investigate the function of endogenous FOSL1, *FOSL1* knockdown was performed in UACC62 cells and gene expression was analyzed by microarray. When a threshold of 1.5-fold regulation was applied, 659 genes were differentially expressed in *FOSL1* knockdown cells compared to control siRNA-treated cells (Figure 3a). Functional clustering by DAVID (<http://david.abcc.ncifcrf.gov/home.jsp>) revealed one biological process, which was markedly enriched (Figure 3b). This group was termed 'neurological system process' and included genes encoding for typical neuronal structure proteins (*NEFL*, *TUBB3*) as well as receptors (*NRP1*). Regulation of these genes by FOSL1 was confirmed in independent knockdown experiments using UACC62 and MelHo cells (Figure 3c and Supplementary Figure 2B). Conversely,

NEFL, *TUBB3* and *NRP1* were upregulated in FOSL1-overexpressing UACC62 and MelHo cells (Figure 3d). As FOSL1 expression strongly depends on MAPK and PI3K pathways, we inhibited these pathways and also observed a reduction of *NEFL*, *NRP1* and *TUBB3* (Figure 3e).

Chromatin remodeling factor HMGA1 is a target of FOSL1

The expression of neuronal genes in melanomas has been described previously.^{26,27} This is considered to be the result of a backslide into earlier developmental stages, as melanocytes, being the precursors of melanoma cells, as well as neuronal cells are derived from the neural crest. Neural crest cells share many features with embryonic stem (ES) cells.²⁸ Interestingly, gene ontology analysis of our gene expression data produced a small group of genes under the gene ontology term 'transcription activator activity', which included the high mobility group member HMGA1. HMGA1 is a chromatin architectural transcription factor, which drives stem cell properties in cancer²⁹ and blocks the differentiation of human ES cells.³⁰

Like FOSL1, HMGA1 is expressed in most melanoma cells at higher protein level compared to NHEM (Supplementary Figure 3A). *FOSL1* knockdown in three different melanoma cell lines caused the reduction of HMGA1 on protein and RNA level (Supplementary Figure 3B–D), and also the inhibition of MEK and PI3K led to a reduction of HMGA1 on both RNA and protein level (Supplementary Figure 3E).

HMGA1 is vital for melanoma cells, as its knockdown (Figure 4a) resulted in strongly reduced proliferation (Figure 4b), impaired two- and three-dimensional colony formation (Figures 4c and d), and reduced cellular survival (Figure 4e).

Of note, FOSL1 overexpression was unable to rescue any of the effects caused by *HMGA1* knockdown, indicating that HMGA1 is a crucial downstream mediator of FOSL1-dependent tumor cell

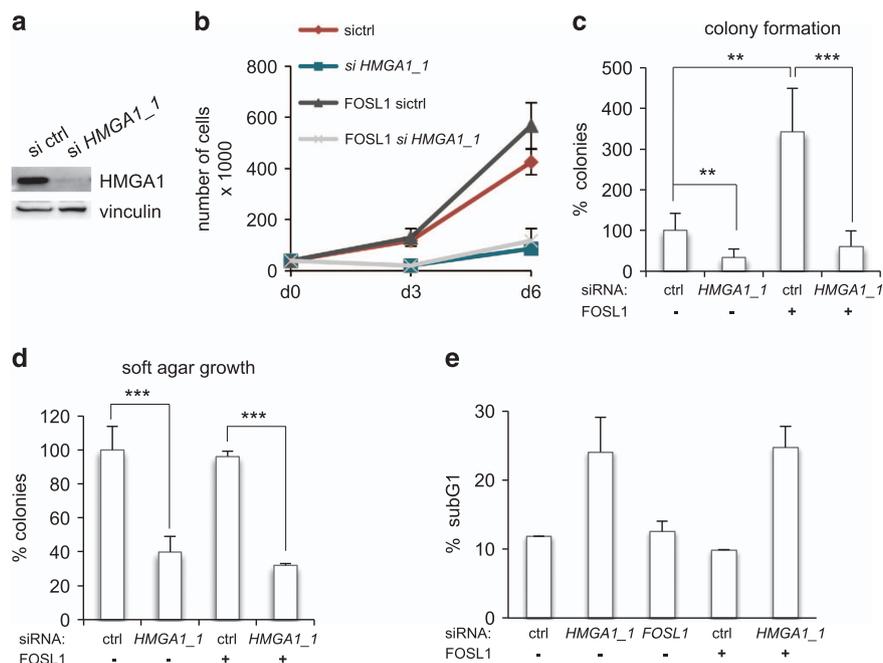


Figure 4. *HMGA1* knockdown suppresses tumor features in melanoma cells. **(a)** Western blot of HMGA1 in UACC62 cells after siRNA mediated gene knockdown with smartpool siRNS (*siHMGA1_1*, 3 days). Vinculin served as loading control. **(b)** Proliferation assay of control and FOSL1 overexpressing UACC62 cells after siRNA mediated knockdown of *HMGA1*. Cells were counted after 3 and 6 days. The experiment was performed two times in triplicates. **(c)** Quantification of 2D-colony formation of control and FOSL1 overexpressing UACC62 cells after siRNA mediated knockdown of *HMGA1*. Cells were cultivated for 12 days. **(d)** Quantification of soft agar growth of control and FOSL1 overexpressing UACC62 cells after siRNA-mediated knockdown of *HMGA1* compared to control siRNA-treated cells, respectively. Cells were allowed to grow for 7 days. Calculations were made from two different biological experiments, each performed in triplicates. **(e)** Quantification of cell death in control and FOSL1 overexpressing UACC62 cells after siRNA-mediated knockdown of *HMGA1*. Cells were fixed 3 days after siRNA-mediated knockdown, stained with propidium iodide and analyzed by flow cytometry. The experiment was performed twice. ****P* < 0.01; *****P* < 0.001.

maintenance (Figures 4b–e). These effects were confirmed with an independent siRNA (Supplementary Figure 4).

Melanocytes undergo transformation upon *FOSL1* expression

As the regulation of neuronal genes by *FOSL1* is reminiscent of the presence of early neural crest-associated developmental features

in the affected melanoma cells, we hypothesized that in turn differentiation features of the melanocytic lineage are reduced by *FOSL1*. We tested this hypothesis using the differentiated melanocyte cell line melan-a. Usually, these cells require the mitogen TPA for growth. We generated a Dox-inducible transposase-based expression vector for *FOSL1*

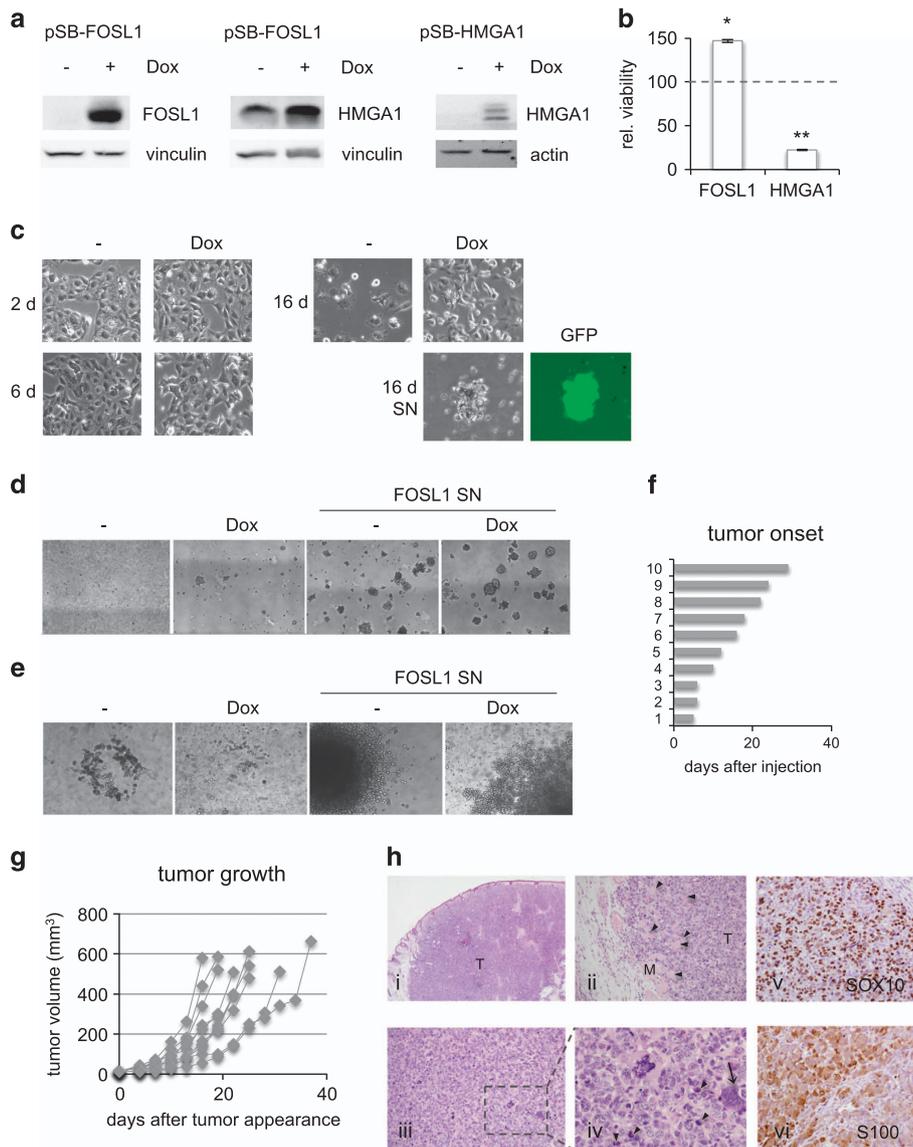


Figure 5. *FOSL1* expression causes anchorage-independent growth and tumor transformation in melanocytes. **(a)** Protein blot demonstrating *FOSL1* and *HMG1A1* expression of melan-a-pSB-*FOSL1* and melan-a-pSB-*HMG1A1* cells, respectively, in response to Dox treatment (1 µg/ml). Vinculin or actin served as loading control. **(b)** Viability MTT assay of melan-a-pSB-*FOSL1* and melan-a-pSB-*HMG1A1* cells in presence of 1 µg/ml Dox, grown for 3 days. Graphs show the change in viability relative to the untreated condition (without Dox), which was set as 100%. Data show the mean of two independent experiments, each performed in triplicate. **P* < 0.05; ***P* < 0.01 **(c)** Appearance of the melan-a-pSB-*FOSL1* cells after 2, 6 and 16 days of cultivation in D10 medium with and without Dox. After 16 days, untreated cells undergo cell death due to the lack of TPA. Dox-induced cells survive as attached cells, but also as detached cells. '16 days SN' designates the cell supernatant of melan-a-pSB-*FOSL1* cells after 16 days of Dox stimulation. The grey image shows phase contrast pictures. As reporter, enhanced GFP is located behind the inducible gene, separated by an internal ribosomal entry site. The green image shows GFP expression of the pSB-*FOSL1* construct. SN: supernatant. **(d)** Soft agar growth of melan-a-pSB-*FOSL1* cells as well as *FOSL1*-SN cells in presence and absence of Dox. Cells were allowed to grow for 14 days. **(e)** Spheroid assay of melan-a-pSB-*FOSL1* cells as well as *FOSL1*-SN cells in presence and absence of Dox. Pictures show the appearance of cells 8 days after embedding into collagen. In **(c–e)**, representative examples of at least three experiments are shown. **(f–h)** Growth of *FOSL1*-SN cells in nude mice. **(f)** Tumor onset in the 10 experimental mice after tumor cell injection. **(g)** Development of tumor volume with time. **(h)** Hematoxylin/eosin staining of tumor tissue sections: (i) shows the location of the tumor with adjacent epidermis. T: tumor. (ii) Tumor infiltration of subcutaneous muscle (20-fold magnification). Arrowheads indicate infiltrated muscle fibres. M: muscle, T: tumor. (iii) Overview of tumor-containing giant multinucleated cells and several mitoses (20-fold magnification). (iv) Magnification of the region indicated in (iii). Arrow and arrowheads indicate a giant tumor cell and mitotic tumor cells, respectively. (v) SOX10 and (vi) S100 staining of the tumor tissue (40-fold magnification).

(pSB-FOSL1) and produced stable transgenic melan-a cells (Figure 5a, left). As expected, FOSL1 induced the expression of HMGA1 (Figure 5a, middle). As controls, we therefore also generated melanocytes stably expressing HMGA1 (pSB-HMGA1; Figure 5a, right).

To investigate the cellular effects of the transcription factors on the melanocytes, we omitted TPA from the medium and investigated the viability in response to FOSL1 or HMGA1 induction. We found that FOSL1 enhanced viability of melan-a cells by almost 50%, whereas HMGA1 had an unexpected suppressive effect (Figure 5b). Long-term propagation was not possible for melan-a-pSB-HMGA1 cells. In contrast, the expression of FOSL1 overcame the growth exhaustion, which otherwise affects the melanocytes after 2 weeks of cultivation in absence of TPA (Figure 5c). Surprisingly, we observed that a substantial number of FOSL1-expressing melanocytes detached from the culture dish after 2 weeks of FOSL1 induction and stayed viable, as shown by their organization as cell clusters and the ability for growth after re-plating (Figure 5c, 16 days SN). They lacked pigmentation and MITF expression (Supplementary Figure 5A and B) and were able to continue proliferation under non-attachment conditions, suggesting that FOSL1 has severely altered the melanocytes. To find out whether this went along with the further gain of pro-tumorigenic features, we used normal melan-a FOSL1 cells as well as the anikis-resistant cells from the supernatant of melan-a FOSL1 cells after 16 days of stimulation with Dox, termed 'FOSL1-SN' cells. Both were seeded in soft agar to detect anikis-independent growth. After 2 weeks of cultivation, melan-a FOSL1 cells were not able at all to form soft agar colonies in the absence of Dox. However, when FOSL1 expression was induced by Dox, few colonies appeared. FOSL1-SN cells, derived from the supernatant of long-term Dox-stimulated melan-a FOSL1 cells, were able to form large soft agar colonies, even when Dox was withdrawn (Figure 5d). Similarly, FOSL1-SN cells were able to form spheroids in a three-dimensional collagen matrix with and without Dox (Figure 5e). However, colonies were larger and less compact when Dox treatment was continued. Melan-a FOSL1 cells were not able to form spheroids, irrespective of FOSL1 expression.

The fact that FOSL1 expression was no longer needed for growth in both *in vitro* assays suggests that FOSL1 has reprogrammed melan-a cells prior to the detachment process. Accordingly, FOSL1-SN cells proved to be tumorigenic in a nude mouse model and gave rise to subcutaneous tumors in 10/10 injected mice, even though Dox was not supplemented (Figures 5f–h) and FOSL1 expression was therefore low (Supplementary Figure 5C). Of note, parental melan-a cells are non-tumorigenic and only give rise to subcutaneous nevi.²⁷ FOSL1-driven tumors were unpigmented, and histological analyses revealed numerous signs of undifferentiated and malignant tumor features, such as invasion of neighboring muscle tissue (Figure 5hi, ii) and the presence of mitotic cells with occasional pleomorphic appearance (Figure 5h). The strong expression of SOX10 and S100 confirmed that the tumors are classified as melanomas (Figure 5h). Metastatic lesions, for example, to the lung, were not detected. In humans, one-third of melanomas are derived from nevi, while the remaining proportion is of unknown origin and can e.g. be derived from skin-residential melanocytes. The fact that FOSL1 is expressed in melanoma, but not in nevi (Figure 2a) or skin, as documented by the protein atlas database (<http://www.proteinatlas.org/ENSG00000175592-FOSL1/tissue>), supports our observation that FOSL1 is instrumental in melanocyte transformation.

Transcriptional reprogramming of melanocytes by FOSL1

To better understand the processes underlying the intriguingly strong oncogenic effect of FOSL1 on melanocytes, we performed

RNASeq analysis of melan-a FOSL1 cells after different time points of Dox treatment: 3 days (initial effects), 16 days (long-term effects), and of FOSL1-SN spheroids. To exclude unspecific effects of Dox on transcription, we also analyzed melan-a cells expressing the pSB control vector in absence or presence of Dox treatment for 3 and 16 days. Gene set enrichment analysis (GSEA) analysis using the KEGG pathway gene set revealed that a large number of pathways are regulated by FOSL1 (see Figures 6a for the 3 days Dox treatment and Supplementary Figure 6A for the 16-day Dox treatment). Among the downregulated pathways, the groups 'lysosome' and 'cell adhesion molecules' showed particularly strong enrichment in 3 day- and 16 day- treated samples. The decrease of adhesion molecules explains the observed cellular detachment (see Figure 5c), and was confirmed by real-time PCR of *Col2a1*, *Itgb3*, *Itg8* and *Itg9* (Figure 6b). In accordance with our previous observations of gradual FOSL1-dependent dedifferentiation, the group 'melanogenesis' was also downregulated, and a strong reduction of *Mitf*, *Dct* and *Tyr* was confirmed by real-time PCR (Figure 6c). Melanogenesis genes were still repressed after 16 days of FOSL1 induction and in FOSL1-induced spheroids (Supplementary Figure 6B), with *Mitf* being among the strongest repressed genes in this group. This indicates that FOSL1 is a potent permanent repressor of MITF. As HMGA1 was reported to interfere with differentiation in ES cells,³⁰ we were interested to find out if it could also affect melanocyte differentiation. Indeed, siRNA-mediated reduction of *HMGA1* partially prevented the FOSL1-mediated reduction of MITF on RNA and protein level, which also affected the MITF target genes *Dct* and *Tyr* (Supplementary Figures 6 C and D).

We furthermore asked the question if FOSL1 regulates the MITF antagonist AXL. It has been observed in numerous cancer cell lines that MITF and AXL expression levels are negatively correlated. Melanoma cells with MITF^{low}/AXL^{high} phenotype show particularly malignant features and are associated with drug resistance against targeted melanoma therapy.³¹ AXL is part of a conserved YAP gene signature, which is strongly enriched in FOSL1-stimulated melanocytes (Figure 6d, left). Indeed, AXL was clearly induced in a FOSL1-dependent manner on RNA and protein level (Figure 6d, right), thus showing that FOSL1 can shift the balance between MITF and AXL.

The pathways most strongly upregulated by FOSL1 affect cell cycle and proliferation-relevant pathways ('cell cycle', 'DNA replication', 'pyrimidine metabolism') as well as transcription/translation and protein-relevant processes ('ribosome', 'spliceosome', 'Parkinson's disease', 'Huntington's disease', 'nucleotide excision repair'). The largest functional group with the highest normalized enrichment score was 'ribosomes'. Again, this group was enriched under all conditions of FOSL1 expressions (3 days, 16 days, spheroids) and was confirmed by real-time PCR (Figure 6e, Supplementary Figure 6B), indicating that FOSL1 constantly enhances ribosome generation. Transmission electron micrographs of melan-a FOSL1 cells revealed an increase in the average number of nucleoli per nuclear section (Figure 6e, right). In addition, nucleoli often appeared larger and more organized when FOSL1 was activated (Supplementary Figure 7A). The number of active nucleoli can be visualized with fibrillarin, a 2'-O-methyltransferase, which locates to the dense fibrillar component of the nucleus.³² We performed immunofluorescence staining for fibrillarin and could detect a significant higher number of fibrillarin spots per cell in Dox-treated melan-a FOSL1 cells compared to their controls (Supplementary Figure 7B). These data indicate that ribosome biogenesis is enhanced by FOSL1.

The information of the FOSL1-dependent processes in melanocytes can be used to identify inhibitors that counteract FOSL1 action. As 'ribosomes' and 'pyrimidine metabolism' belong to pathways, whose members can be inhibited by well-defined substances available in the clinic, we chose inhibitors for both groups to test whether the growth advantage of FOSL1-

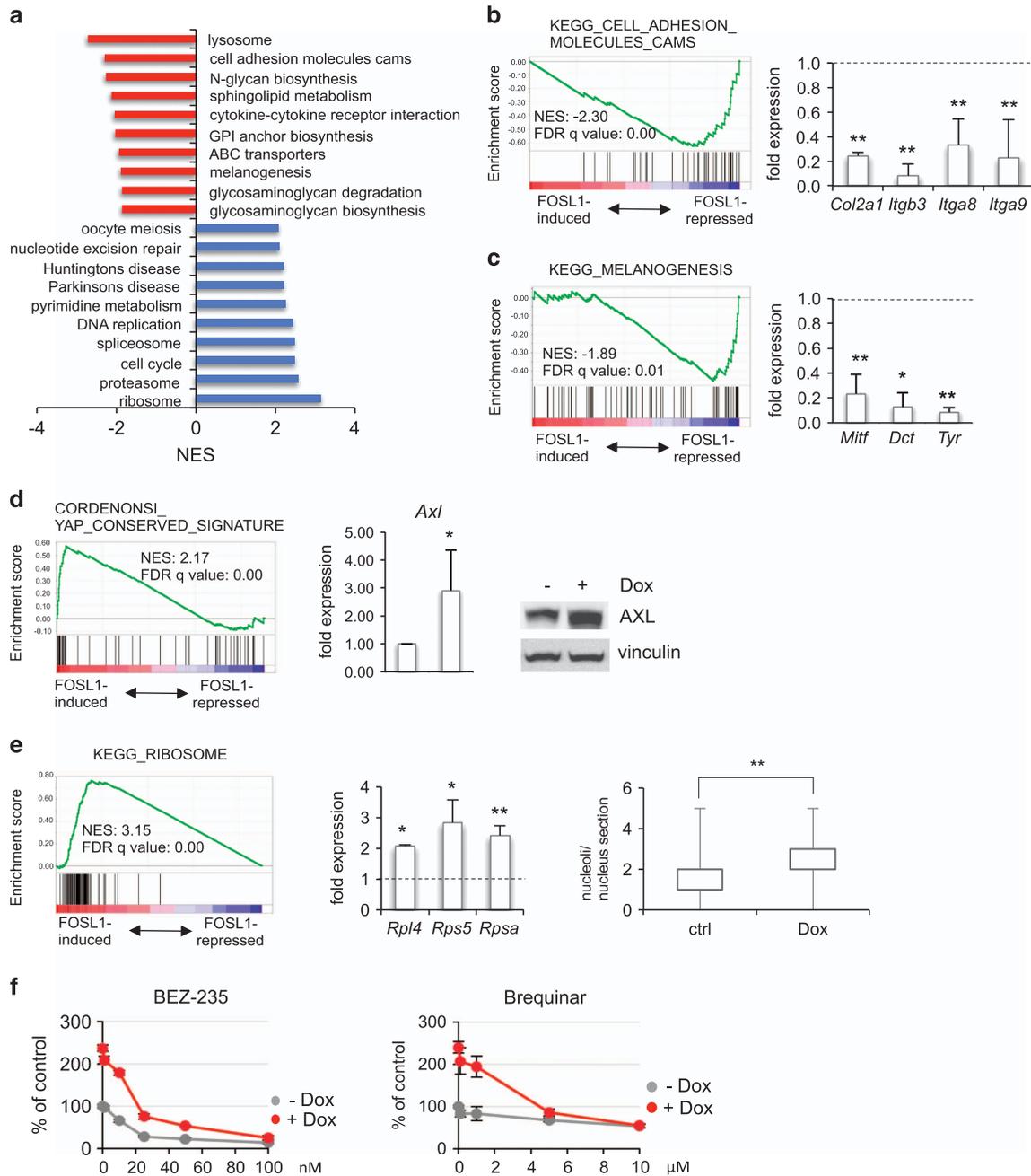


Figure 6. Dedifferentiation and cellular reprogramming by FOSL1. **(a)** Functional characteristics of altered transcripts in melanocytes after induction of FOSL1 (3 days), as revealed by GSEA analysis (KEGG pathways). NES: Normalized enrichment score. **(b, left):** GSEA enrichment plot of the KEGG pathway 'cell adhesion molecules cams'. **Right:** Real-time PCR analysis of *Col2a1*, *Itgb3*, *Itga8* and *Itga9* in melan-a FOSL1 cells after Dox treatment for 3 days. **(c, left)** GSEA enrichment plot of the KEGG pathway 'melanogenesis'. **Right:** Real-time PCR analysis of *Mitf*, *Dct* and *Tyr* in melan-a FOSL1 cells after Dox treatment for 3 days. Untreated melan-a FOSL1 cells served as control and were set as 1. **(d)** Left: GSEA enrichment plot of the gene set 'Cordenonsi YAP conserved signature' in melan-a FOSL1 cells after 3 days of FOSL1 induction. Middle: Real-time PCR analysis and protein blot (right) showing increased expression of *Axl* RNA and AXL protein in response to a 3-day FOSL1 induction. **(e, left):** GSEA enrichment plot of the KEGG pathway 'ribosome'. Middle: Real-time PCR analysis of *Rpl4*, *Rps5* and *Rpsa* in melan-a FOSL1 cells after Dox treatment for 3 days. **Right:** Boxplot, showing the quantification of the average number of counted nucleoli per nucleus in transmission electron micrograph sections. For each condition, 100 nuclei were analyzed. In the boxplot figure, the median value (in the box), the first and third quartile (upper and lower border of the box), and the minimum and maximum values are indicated. Significance was calculated using Student's *t* test (unpaired). **(f)** Viability MTT assay of melan-a-pSB-FOSL1 cells in absence or presence of 1 μg/ml Dox, and indicated concentrations of BEZ-235 and brequinar, grown for 5 days. Graphs show the change in viability relative to the untreated condition (without Dox), which was set as 100%. **P* < 0.05; ***P* < 0.01.

expressing melanocytes can be blocked. Ribosome biogenesis is regulated by the mTOR pathway³³ and can be blocked by the PI3K/mTOR inhibitor BEZ-235 ('dactolisib'), which is in clinical trials for the treatment of different solid or hematological cancer types.

Pyrimidine metabolism can be inhibited by brequinar, which specifically blocks the dihydroorotate dehydrogenase and has anti-tumor and immunosuppressive effects. When we cultivated melan-a FOSL1 cells for 5 days in absence or presence of Dox, we

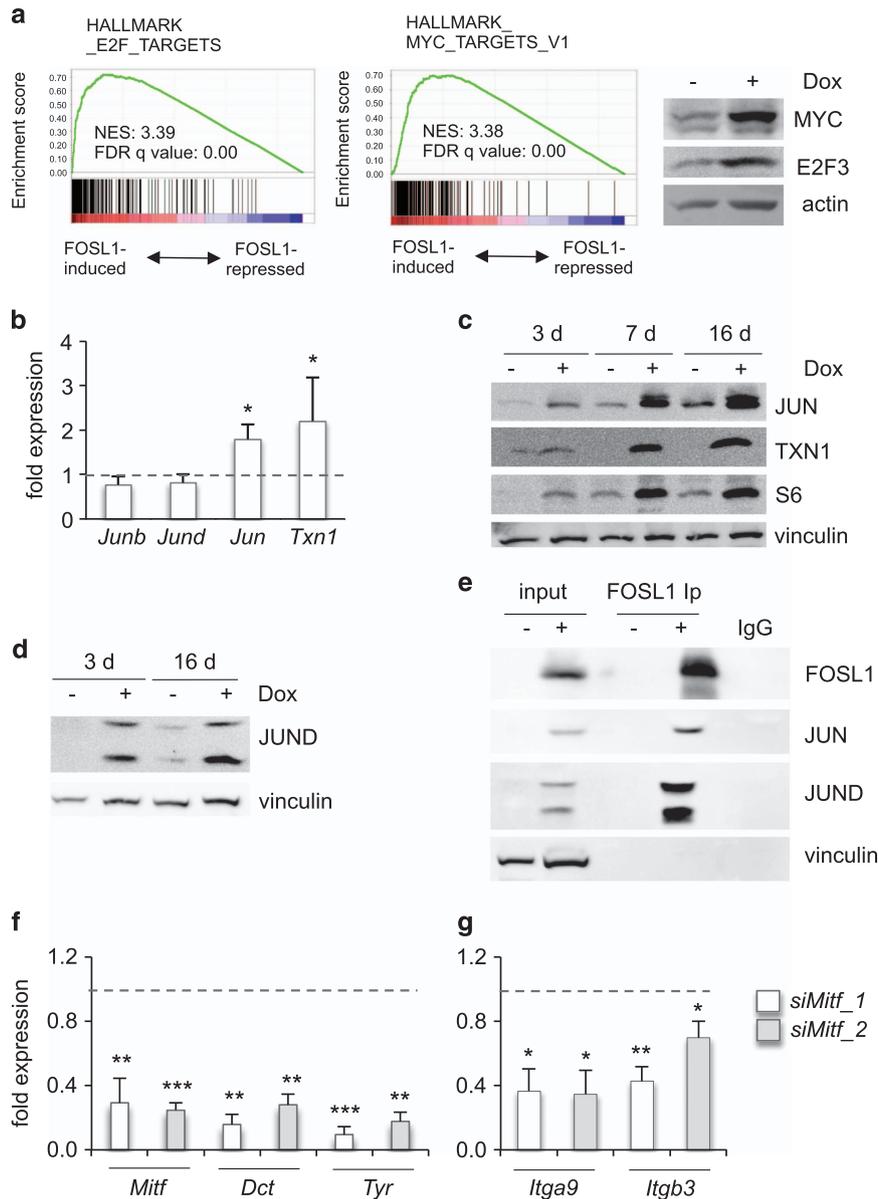


Figure 7. Induction and maintenance of oncogenic transcription factors by FOSL1. (a, left): GSEA enrichment plot of the HALLMARK gene sets 'E2F targets' and 'MYC targets V1'. Right: Protein blot showing enhanced expression of c-MYC and E2F3 after FOSL1 induction in melan-a FOSL1 cells (3 days). (b) Real-time PCR analysis of *Junb*, *Jund*, *Jun* and *Txn1* in melan-a FOSL1 cells after Dox treatment for 3 days. Untreated melan-a FOSL1 cells served as control and were set as 1. (c) Protein blot showing enhanced expression of JUN, TXN1, and S6 ribosomal protein after FOSL1 induction in melan-a FOSL1 cells for indicated time points. Vinculin served as loading control. (d) Protein blot showing enhanced expression of JUND after FOSL1 induction in melan-a FOSL1 cells for indicated time points. Vinculin or actin served as loading control. (e) Immunoprecipitation of melan-a FOSL1 cells stimulated for 3 days with Dox (+) or left unstimulated (-). Four hundred micrograms protein lysate were used for immunoprecipitation, using FOSL1-specific antibody. As control, 40 µl of input was applied. The blot was probed for FOSL1, JUN, JUND and vinculin. (f), (g) Real-time PCR of *Mitf*, *Dct* and *Tyr* (f) or *Itga9* and *Itgb3* (g) in melan-a cells transfected with two different siRNAs targeting *Mitf*. * $P < 0.05$; ** $P < 0.01$; *** $P < 0.001$.

observed a strong FOSL1-dependent growth stimulation, which was blocked by BEZ-235 as well as brequinar (Figure 6f).

Manifestation of FOSL1 effects by transcriptional task allocation

Apart from the involvement of FOSL1-regulated genes in functional KEGG pathways, we were interested in the question if FOSL1 activates potent downstream effectors, which support its effect. When we applied the GSEA hallmark gene set, the top two highly enriched gene groups (with normalized enrichment score values > 3.3) were 'E2F targets' and 'MYC targets' (Figure 7a, left). In line with these data, we observed the induction of c-MYC and E2F3 on

protein level (Figure 7a, right). E2F3 is a regulator of cell cycle genes, while c-MYC controls the expression of a large set of the cellular transcriptome, including cell cycle genes, ribosomal genes (which are upregulated by MYC) and integrins (which are repressed by MYC).³⁴ As similar gene regulations are mediated by FOSL1, we suggest that at least some of the observed effects are caused by MYC and E2F3.

To test if FOSL1 is able to influence its own interaction partners and thereby alter AP-1 availability, we specifically investigated gene expression of the most common AP-1 interaction partners, namely *Junb*, *Jund*, *Jun* as well as thioredoxin 1 (*Txn1*), which was previously reported to play an important role in AP-1

transcription factor activity.³⁵ While *Junb* and *Jund* RNA levels remained unaffected, FOSL1 increased the transcription of *Jun* and *Txn1* (Figure 7b). This increase was confirmed on protein level (Figure 7c). Notably, the long-term induction of FOSL1-inducing oncogenes BRAF^{V600E} and NRAS^{Q61K} in NHEM cells also resulted in elevated JUN and TXN1 (Supplementary Figure 8C). NRAS^{Q61K} showed a stronger effect on both proteins than BRAF^{V600E}, which coincides with its higher induction of FOSL1 (see Supplementary Figure 1A).

In melan-a cells, JUN expression became stronger with time of FOSL1 induction, along with the ribosomal marker S6 ribosomal protein (Figure 7c). As the increase of ribosomal biogenesis might affect protein expression without altering gene expression, we also tested protein expression of JUNB and JUND. JUNB was hardly expressed (data not shown), but JUND was increased after long-term FOSL1 stimulation (Figure 7d). Immunoprecipitation experiments confirmed that FOSL1 was able to interact with both JUN and JUND (Figure 7e).

To better understand the role of FOSL1-mediated dedifferentiation in the processes accompanying transformation, we investigated the effect of MITF reduction in melan-a cells. Normal melan-a cells were kept in absence of TPA, and *Mitf* was knocked down using two different siRNAs. As expected, the differentiation genes *Dct* and *Tyr* were strongly reduced under these conditions (Figure 7f). Interestingly, we also observed a clear downregulation of integrins (Figure 7g), whereas the MITF knockdown had no effect on AXL and ribosomal markers (Supplementary Figure 8A and B).

These data demonstrate that FOSL1 is an efficient modulator of downstream transcriptional programs, which are associated with tumorigenic features and manifest the malignant character of the cells.

DISCUSSION

In this study, we explored the functional role of the AP-1 transcription factor component FOSL1 in melanoma cells and untransformed melanocytes. In contrast to epithelial cancer types, where FOSL1 is involved in epithelial-to-mesenchymal transition and consequently invasion and metastasis,^{16–18} FOSL1 has additional functions in melanoma cells and melanocytes. It is involved in proliferation, anoikis resistance and migration. We found that the endogenous FOSL1 level in melanoma is jointly maintained by PI3K and MAPK pathways. This demonstrates that although *FOSL1* is a typical MAPK-dependent immediate early gene, MAPK pathway activation alone is not sufficient to keep up FOSL1 levels. In mouse models and human tumors, activation of the PI3K pathway on top of MAPK pathway activation is associated with the progression of melanocytic precursor lesions to melanoma.^{21–23} Similarly, FOSL1 expression is increased in melanomas in comparison to nevi. To test if this observation is purely correlative or if FOSL1 can affect melanocyte transformation, we expressed FOSL1 in non-transformed melanocytes and found surprisingly that FOSL1 expression was fully able to cause the generation of tumors. FOSL1 re-organized the transcriptional landscape of melanocytes and led to melanocyte reprogramming, which was most obvious by the visible loss of melanocyte differentiation (summarized in Supplementary Figure 8D). We identified strong and consistent repression of MITF by FOSL1 in melanocytes in a HMGA1-dependent manner. Due to its global effect on chromatin rearrangement, it is, however, likely that HMGA1 fulfills further tasks in addition to MITF repression. MITF is specifically expressed in cells of the pigment cell lineage, such as melanocytes and melanoma cells. It serves many tasks and was described to have pro-tumorigenic as well as anti-tumorigenic effects in melanoma cells.³⁶ Generally, high MITF expression seems to favor proliferation, while low MITF levels favor invasion in fully transformed melanoma cells.^{24,37} Notably, decreasing

MITF levels using a temperature sensitive unstable MITF version causes the generation of melanoma in zebrafishes harboring a melanocyte-specific BRAF-mutant, whereas BRAF^{V600E} alone only gives rise to nevi.³⁸ This indicates that reduced MITF activity favors the generation of melanoma from previously untransformed cells. However, MITF is also important for melanoma survival. In agreement with this observation, even long-term FOSL1 stimulation of melanocytes led to a strong reduction, but not the abolishment of MITF expression in our experiments. Apart from the observed dedifferentiation, which is accompanied by reduction of ‘classical’ MITF targets *Dct* and *Tyr*, MITF repression affected the expression of integrins in the melan-a FOSL1 cells, thus suggesting an effect on migration or invasion, which will be the subject of future studies. Furthermore, it was previously described that MITF serves as major inducer of lysosomal biogenesis,³⁹ and accordingly, the KEGG pathway with the strongest downregulation in melanocytes with activated FOSL1 and repressed MITF is termed ‘lysosome’ (Figure 6a, Supplementary Figure 6A). FOSL1-dependent downregulation of MITF is particularly interesting in the context of simultaneous AXL induction and sheds new light on several aspects of melanoma biology. MITF and AXL are inversely correlated in melanoma cell lines and melanomas, and MITF^{low}; AXL^{high} melanoma cells are devoid of differentiation markers, but show enhanced invasive potential and a high degree of resistance towards targeted therapy.^{31,40} The MITF^{low}; AXL^{high} signature could recently be confirmed by single-cell RNASeq analysis from freshly isolated metastatic melanomas by Tirosh and colleagues.⁴¹ Importantly, the authors showed that FOSL1 is on top of the gene signature which goes along with the AXL^{high} phenotype (Supplementary Table 8 from Tirosh *et al.*,⁴¹), strongly supporting that FOSL1 is responsible for shifting the balance between MITF and AXL.

A remarkable feature of FOSL1 is the enforcement of several transcription factors, such as c-MYC, E2F3 as well as AP-1, which guarantees strong transcriptional effects as long as FOSL1 is expressed. Accordingly, transcriptional effects of FOSL1 strongly overlap with those of c-MYC and E2F3. MYC is an efficient inducer of ribosomal biogenesis and the resulting translation efficiency and thereby increases the production of downstream targets even in absence of transcriptional control.³⁴ We made similar observations in FOSL1-expressing melanocytes, which show a robust induction of protein abundance of several proteins over time. In addition, MYC profoundly represses cell surface molecules, such as integrins and matrix components, similar to FOSL1 and MITF.³⁴ E2F3 is mostly responsible for inducing cell cycle genes, thereby stimulating cell cycle progression and mitosis,⁴² a feature also shared by FOSL1. Interestingly, genes with E2F binding sites often contain additional TEAD consensus sites.⁴³ TEADs such as TEAD4 are transcription factors serving as bridging partners between AP-1 factors and YAP/TAZ, thereby regulating pro-tumorigenic gene expression.⁴⁴ Given the fact that the FOSL1 gene signature entails a large group of YAP/TAZ target genes, it is likely that this transcription factor complex interacts with FOSL1.

Our analyses reveal that FOSL1 plays a special role in melanoma development, which is different from that of other cancer types, presumably because of its effect on the lineage-specific transcription factor MITF.

MATERIALS AND METHODS

Cell culture

UACC62, SKMEL-2 and M14 cells are part of the NCI-60 panel and were received from the NCI/NIH (DCTD Tumor Repository, National Cancer Institute at Frederick, Frederick, Maryland). SKMEL-28 and A375 were purchased from ATCC. Melanoma cell lines were authenticated using the PowerPlex 16 DNA typing system (Promega, Mannheim, Germany). All melanoma cell lines were cultivated in Dulbecco’s modified Eagle medium supplemented with 10% fetal calf serum and 1 × penicillin/streptomycin

(Sigma, Taufkirchen, Germany) at 37 °C and 5% CO₂. NHEM cells, purchased from Promocell (Heidelberg, Germany), were maintained in Ham's F10 containing 20% fetal calf serum, 100 nM TPA (Calbiochem/Merck, Darmstadt, Germany), 200 pM cholera toxin (Calbiochem), penicillin/streptomycin, 100 μM 3-isobutyl-1-methylxanthine and ITS Premix (1:1000 BD Biosciences, Heidelberg, Germany). Murine melanocytes ('melan-a') were originally isolated in the laboratory of Dorothy Bennett (St George's, University of London, London, UK) and were obtained from the Wellcome Trust Functional Genomic Cell Bank (St George's, University of London). For cell culture expansion, they were kept in Dulbecco's modified Eagle medium containing 10% fetal calf serum, 200 nM TPA, 12 nM cholera toxin (Calbiochem), penicillin/streptomycin. Human colon carcinoma cells were grown in RPMI medium containing 10% fetal calf serum and 1 × penicillin/streptomycin (Sigma). The MEK inhibitor PD184352 was purchased from Axon Medchem (Groningen, The Netherlands). Nutlin3a and GDC0941 were acquired from Selleckchem (Munich, Germany).

siRNA transfection

Cells were treated with either commercially available siRNA against human *FOSL1*, (siGENOME SMARTpool, Thermo Scientific (Dreieich, Germany), and Mission single siRNA's, Sigma), human and murine *HMG1* (human siGENOME SMARTpool HMG1, Thermo Scientific, and one or two different Mission single siRNA's, Sigma for human and mouse, respectively), murine *Mitf* (with two different Mission single siRNA's, Sigma) as well as control siRNA (ON-Target plus Non-Targeting pool, Thermo Scientific, and Mission non-targeting siRNA). X-treme gene transfection reagent (Roche, Mannheim, Germany) was applied for transfection according to the manufacturer's recommendation. The following day, cells were reseeded for further experiments.

Proliferation assay

Cells were seeded in triplicates onto six-well plates at defined cell numbers. After 3 and 6 days, cells were harvested, resuspended in PBS and counted using a Neubauer hemocytometer.

RNA extraction, cDNA synthesis and qPCR

RNA and miRNA isolation was performed using TRIzol reagent (Life Technologies, Darmstadt, Germany) according to the manufacturer's protocol. DNA digestion was performed with DNase I for 1 h at 37 °C (Thermo Scientific). Subsequently, RNA was reversely transcribed with a RevertAid First Strand cDNA Synthesis Kit (Fermentas, Dreieich, Germany). Fluorescence-based RT-qPCR was performed and analyzed with a Mastercycler ep Realplex from Eppendorf using SYBR Green reagent. Gene expression was normalized to *RPS14* (human cells) and *Actb* (mouse cells), both remaining unaltered under the treatment conditions. Oligonucleotide sequences are indicated in Supplementary Table 1.

Cell lysis and western blot

Cells were lysed in lysis buffer (20 mM HEPES (pH 7.8); 500 mM NaCl, 5 mM MgCl₂, 5 mM KCl; 0.1% deoxycholate, 0.5% Nonidet-P40; 10 μg/ml aprotinin; 10 μg/ml leupeptin; 200 μM Na₂VO₄; 1 mM phenylmethanesulphonyl-fluoride and 100 mM NaF). 40 μg of protein was separated by sodium dodecyl sulfate polyacrylamide gel electrophoresis and was analyzed by western blotting. Antibodies directed against β-actin, p53, BRAF, ERK2, NRAS, MYC, E2F3 and AXL were from Santa Cruz Biotechnology (Heidelberg, Germany). Antibodies targeting HMG1, α-tubulin and vinculin were obtained from Sigma. Antibodies detecting P-AKT (Ser473), total AKT, P-ERK1/2 (Thr202/Tyr204), P-p53 (Ser15), FOSL1, JUN, JUND, thioredoxin, cleaved PARP and S6 ribosomal protein were received from Cell Signaling (Leiden, The Netherlands). The MITF antibody was a gift from C. Goding (Oxford Ludwig Institute, University of Oxford).

Microarray analysis

UACC62 cells were harvested 72 h after transfection with either siRNA-targeting *FOSL1* or non-targeting control siRNA. RNA was extracted using the RNeasy kit from Qiagen. Thereafter, RNA was hybridized to a GeneChip Human Gene 2.0 ST array (Affymetrix, Dreieich, Germany). Data were analyzed using R (cran.r-project.org). Briefly, data were preprocessed using Robust Multi-array Average and were quantile-quantile normalized. Differential expression was calculated. Genes with a fold change > 1.5 were functionally clustered using the online tool DAVID (<http://david.abcc.ncifcrf.gov/home.jsp>).

Obtained data are available at <http://www.ncbi.nlm.nih.gov/geo/query/acc.cgi?token=mjexqiogpwwzryx&acc=GSE85086> (reviewer link).

RNA-Seq

Melan-a FOSL1 cells and melan-a control cells (carrying pSB-ET-iE) were cultivated in triplicates and were kept for 3 and 16 days in absence or presence of 1 μg/ml Dox. Similarly, spheroids from melan-a FOSL-SN cells kept in absence or presence of 1 μg/ml Dox for 8 days in a three-dimensional collagen matrix were harvested in triplicates. Total RNA was extracted with RNeasy Kit (Qiagen, Hilden, Germany). Before RNASeq analysis, triplicates were pooled. RNA integrity was assessed with a Bioanalyzer 2100 (Agilent, Waldbronn, Germany). RNA integrity numbers (RINs) of RNA pools ranged between 9.3 and 10 (RNA integrity number 10 corresponding to completely intact RNA). Libraries for RNA-Seq samples were constructed using 500 ng total RNA following the manufacturer's instructions using the TruSeq stranded mRNA kit (Illumina, Eindhoven, The Netherlands) and sequenced on a NextSeq 500 (Illumina). Thirty-two to thirty-nine million strand-specific short reads were obtained for each RNA-Seq library. Library preparation and sequencing was performed at the Core Unit Systems Medicine at the University of Würzburg. RNA-Seq data are deposited at the SRA repository (NCBI, accession number SUB1734137).

Statistical analysis

Unless indicated otherwise, the graphs depict the mean values of at least three independent experiments, and standard deviations are indicated. Student's *t*-test (two-tailed, unpaired) revealed statistical significance highlighted by asterisks (**P* < 0.05; ***P* < 0.01, ****P* < 0.001). In all cases, indicated error bars represent standard deviations.

CONFLICT OF INTEREST

The authors declare no conflict of interest.

ACKNOWLEDGEMENTS

This work was supported by the Melanoma Research Network of the Deutsche Krebshilfe eV (German Cancer Aid) and by the research unit FOR2314, project 5 (German Research Foundation). We are furthermore grateful to Manfred Gessler (Dept of Developmental Biochemistry, University of Würzburg) for providing us with the pSB-ET-iE vector and to Stefan Gaubatz (Dept. of Physiological Chemistry, University of Würzburg) for the E2F3 antibody. We would also like to thank Marie-Christine Dabauvalle (Dept of Zoology and Developmental Biology, University of Würzburg) for sharing the fibrillarlin antibody with us.

REFERENCES

- Mandal R, Becker S, Strebhardt K. Stamping out RAF and MEK1/2 to inhibit the ERK1/2 pathway: an emerging threat to anticancer therapy. *Oncogene* 2016; **35**: 2547–2561.
- Vogt PK. Fortuitous convergences: the beginnings of JUN. *Nat Rev Cancer* 2002; **2**: 465–469.
- Lopez-Bergami P, Kim H, Dewing A, Goydos J, Aaronson S, Ronai Z. c-Jun regulates phosphoinositide-dependent kinase 1 transcription: implication for Akt and protein kinase C activities and melanoma tumorigenesis. *J Biol Chem* 2010; **285**: 903–913.
- Riesenberg S, Groetchen A, Siddaway R, Bald T, Reinhardt J, Smorra D *et al*. MITF and c-Jun antagonism interconnects melanoma dedifferentiation with pro-inflammatory cytokine responsiveness and myeloid cell recruitment. *Nat Commun* 2015; **6**: 8755.
- Kappelmann M, Kuphal S, Meister G, Vardimon L, Bosserhoff AK. MicroRNA miR-125b controls melanoma progression by direct regulation of c-Jun protein expression. *Oncogene* 2013; **32**: 2984–2991.
- Spangler B, Vardimon L, Bosserhoff AK, Kuphal S. Post-transcriptional regulation controlled by E-cadherin is important for c-Jun activity in melanoma. *Pigment Cell Melanoma Res* 2011; **24**: 148–164.
- Spangler B, Kappelmann M, Schitteck B, Meierjohann S, Vardimon L, Bosserhoff AK *et al*. ETS-1/RhoC signaling regulates the transcription factor c-Jun in melanoma. *Int J Cancer* 2012; **130**: 2801–2811.
- Cohen DR, Curran T. fra-1: a serum-inducible, cellular immediate-early gene that encodes a fos-related antigen. *Mol Cell Biol* 1988; **8**: 2063–2069.

- 9 Nishina H, Sato H, Suzuki T, Sato M, Iba H. Isolation and characterization of fra-2, an additional member of the fos gene family. *Proc Natl Acad Sci USA* 1990; **87**: 3619–3623.
- 10 Tice DA, Soloviev I, Polakis P. Activation of the Wnt pathway interferes with serum response element-driven transcription of immediate early genes. *J Biol Chem* 2002; **277**: 6118–6123.
- 11 Chinenov Y, Kerppola TK. Close encounters of many kinds: Fos-Jun interactions that mediate transcription regulatory specificity. *Oncogene* 2001; **20**: 2438–2452.
- 12 Shaulian E, Schreiber M, Piu F, Beeche M, Wagner EF, Karin M. The mammalian UV response: c-Jun induction is required for exit from p53-imposed growth arrest. *Cell* 2000; **103**: 897–907.
- 13 Ting CH, Chen YC, Wu CJ, Chen JY. Targeting FOSB with a cationic antimicrobial peptide, TP4, for treatment of triple-negative breast cancer. *Oncotarget* 2016; **7**: 40329–40347.
- 14 Nakabeppu Y, Oda S, Sekiguchi M. Proliferative activation of quiescent Rat-1A cells by delta FosB. *Mol Cell Biol* 1993; **13**: 4157–4166.
- 15 Saez E, Rutberg SE, Mueller E, Oppenheim H, Smoluk J, Yuspa SH *et al*. c-fos is required for malignant progression of skin tumors. *Cell* 1995; **82**: 721–732.
- 16 Desmet CJ, Gallenne T, Prieur A, Reyat F, Visser NL, Wittner BS *et al*. Identification of a pharmacologically tractable Fra-1/ADORA2B axis promoting breast cancer metastasis. *Proc Natl Acad Sci USA* 2013; **110**: 5139–5144.
- 17 Iskit S, Schlicker A, Wessels L, Peeper DS. Fra-1 is a key driver of colon cancer metastasis and a Fra-1 classifier predicts disease-free survival. *Oncotarget* 2015; **6**: 43146–43161.
- 18 Yang S, Li Y, Gao J, Zhang T, Li S, Luo A *et al*. MicroRNA-34 suppresses breast cancer invasion and metastasis by directly targeting Fra-1. *Oncogene* 2013; **32**: 4294–4303.
- 19 Renaud SJ, Kubota K, Rumi MA, Soares MJ. The FOS transcription factor family differentially controls trophoblast migration and invasion. *J Biol Chem* 2014; **289**: 5025–5039.
- 20 Basbous J, Chalbos D, Hipskind R, Jariel-Encontre I, Piechaczyk M. Ubiquitin-independent proteasomal degradation of Fra-1 is antagonized by Erk1/2 pathway-mediated phosphorylation of a unique C-terminal destabilizer. *Mol Cell Biol* 2007; **27**: 3936–3950.
- 21 Dankort D, Curley DP, Cartledge RA, Nelson B, Karnezis AN, Damsky WE Jr *et al*. Braf(V600E) cooperates with Pten loss to induce metastatic melanoma. *Nat Genet* 2009; **41**: 544–552.
- 22 Shain AH, Yeh I, Kovalyshyn I, Sriharan A, Talevich E, Gagnon A *et al*. The Genetic Evolution of Melanoma from Precursor Lesions. *N Engl J Med* 2015; **373**: 1926–1936.
- 23 Vredeveld LC, Possik PA, Smit MA, Meissl K, Michaloglou C, Horlings HM *et al*. Abrogation of BRAFV600E-induced senescence by PI3K pathway activation contributes to melanomagenesis. *Genes Dev* 2012; **26**: 1055–1069.
- 24 Widmer DS, Cheng PF, Eichhoff OM, Belloni BC, Zipser MC, Schlegel NC *et al*. Systematic classification of melanoma cells by phenotype-specific gene expression mapping. *Pigment Cell Melanoma Res* 2012; **25**: 343–353.
- 25 Vincek V, Xu S, Fan YS. Comparative genome hybridization analysis of laser-capture microdissected in situ melanoma. *J Cutan Pathol* 2010; **37**: 3–7.
- 26 Landsberg J, Kohlmeyer J, Renn M, Bald T, Rogava M, Cron M *et al*. Melanomas resist T-cell therapy through inflammation-induced reversible dedifferentiation. *Nature* 2012; **490**: 412–416.
- 27 Leikam C, Hufnagel AL, Otto C, Murphy DJ, Muhling B, Kneitz S *et al*. In vitro evidence for senescent multinucleated melanocytes as a source for tumor-initiating cells. *Cell Death Dis* 2015; **6**: e1711.
- 28 Thomas S, Thomas M, Wincker P, Babarit C, Xu P, Speer MC *et al*. Human neural crest cells display molecular and phenotypic hallmarks of stem cells. *Hum Mol Genet* 2008; **17**: 3411–3425.
- 29 Belton A, Gabrovsky A, Bae YK, Reeves R, Iacobuzio-Donahue C, Huso DL *et al*. HMGA1 induces intestinal polyposis in transgenic mice and drives tumor progression and stem cell properties in colon cancer cells. *PLoS One* 2012; **7**: e30034.
- 30 Shah SN, Kerr C, Cope L, Zambidis E, Liu C, Hillion J *et al*. HMGA1 reprograms somatic cells into pluripotent stem cells by inducing stem cell transcriptional networks. *PLoS One* 2012; **7**: e48533.
- 31 Muller J, Krijgsman O, Tsoi J, Robert L, Hugo W, Song C *et al*. Low MITF/AXL ratio predicts early resistance to multiple targeted drugs in melanoma. *Nat Commun* 2014; **5**: 5712.
- 32 Martin RM, Tunneemann G, Leonhardt H, Cardoso MC. Nucleolar marker for living cells. *Histochem Cell Biol* 2007; **127**: 243–251.
- 33 Gentilella A, Kozma SC, Thomas G. A liaison between mTOR signaling, ribosome biogenesis and cancer. *Biochim Biophys Acta* 2015; **1849**: 812–820.
- 34 Elkon R, Loayza-Puch F, Korkmaz G, Lopes R, van Breugel PC, Bleijerveld OB *et al*. Myc coordinates transcription and translation to enhance transformation and suppress invasiveness. *EMBO Rep* 2015; **16**: 1723–1736.
- 35 Das KC, Muniyappa H. c-Jun-NH2 terminal kinase (JNK)-mediates AP-1 activation by thioredoxin: phosphorylation of cJun, JunB, and Fra-1. *Mol Cell Biochem* 2010; **337**: 53–63.
- 36 Wellbrock C, Arozarena I. Microphthalmia-associated transcription factor in melanoma development and MAP-kinase pathway targeted therapy. *Pigment Cell Melanoma Res* 2015; **28**: 390–406.
- 37 Bianchi-Smiraglia A, Bagati A, Fink EE, Moparthy S, Wawrzyniak JA, Marvin EK *et al*. Microphthalmia-associated transcription factor suppresses invasion by reducing intracellular GTP pools. *Oncogene* 2016; **36**: 84–96.
- 38 Lister JA, Capper A, Zeng Z, Mathers ME, Richardson J, Paranthaman K *et al*. A conditional zebrafish MITF mutation reveals MITF levels are critical for melanoma promotion vs. regression in vivo. *J Invest Dermatol* 2014; **134**: 133–140.
- 39 Ploper D, Taelman VF, Robert L, Perez BS, Titz B, Chen HW *et al*. MITF drives endolysosomal biogenesis and potentiates Wnt signaling in melanoma cells. *Proc Natl Acad Sci USA* 2015; **112**: E420–E429.
- 40 Sensi M, Catani M, Castellano G, Nicolini G, Alciato F, Tragni G *et al*. Human cutaneous melanomas lacking MITF and melanocyte differentiation antigens express a functional Axl receptor kinase. *J Invest Dermatol* 2011; **131**: 2448–2457.
- 41 Tirosh I, Izar B, Prakadan SM, Wadsworth MH 2nd, Treacy D, Trombetta JJ *et al*. Dissecting the multicellular ecosystem of metastatic melanoma by single-cell RNA-seq. *Science* 2016; **352**: 189–196.
- 42 Ren B, Cam H, Takahashi Y, Volkert T, Terragni J, Young RA *et al*. E2F integrates cell cycle progression with DNA repair, replication, and G(2)/M checkpoints. *Genes Dev* 2002; **16**: 245–256.
- 43 Kapoor A, Yao W, Ying H, Hua S, Liewen A, Wang Q *et al*. Yap1 activation enables bypass of oncogenic Kras addiction in pancreatic cancer. *Cell* 2014; **158**: 185–197.
- 44 Zanconato F, Forcato M, Battilana G, Azzolin L, Quaranta E, Bodega B *et al*. Genome-wide association between YAP/TAZ/TEAD and AP-1 at enhancers drives oncogenic growth. *Nat Cell Biol* 2015; **17**: 1218–1227.
- 45 Huang, da W, Sherman BT, Lempicki RA. Systematic and integrative analysis of large gene lists using DAVID bioinformatics resources. *Nat Protoc* 2009; **4**: 44–57.

Supplementary Information accompanies this paper on the Oncogene website (<http://www.nature.com/onc>)